Topic 5: Tests of fundamental theories of physics using black hole systems

https://doi.org/10.1017/S174392131700076X Published online by Cambridge University Press

New Frontiers in Black Hole Astrophysics
Proceedings IAU Symposium No. 324, 2016
Andreja Gomboc, ed.

doi:10.1017/S174392131700076X

Unveiling early black holes with *JWST*

Priyamvada Natarajan

Department of Astronomy, Yale University, 52 Hillhouse Avenue, New Haven, CT 06520, U.S.A.
email: priyamvada.natarajan@yale.edu

Abstract. The formation of direct collapse black hole seeds with masses $\sim 10^4 - 10^5$ $M_\odot$ could help explain the assembly of supermassive black holes powering high redshift quasars. Conditions conducive to the formation of these massive initial seeds exist at high redshift. Halos hosting these massive seeds merge promptly with a nearby galaxy. These early stage mergers at high redshift produce a new class of transient galaxies that contain an accreting black hole that is over-massive compared to the newly acquired stellar component - Obese Black hole Galaxies (OBGs). During this phase, the accretion luminosity of the direct collapse black hole seed exceeds that of the acquired stellar component. Here we calculate the multi-wavelength spectrum of this short-lived OBG stage, and show that there exist unique observational signatures in long wavelengths spanning near, mid to far-infrared that should be detectable by instruments aboard the upcoming James Webb Space Telescope (JWST).

Keywords. black hole physics, cosmology: early universe, infra-red: galaxies

1. Introduction

Discovery of populations of luminous, high redshift quasars at $z \gtrsim 6$, suggests that supermassive black holes with masses of the order 10^{8-10} $M_\odot$ are already in place at these early epochs in the universe as reported in observations by Fan *et al.* (2001), Mortlock *et al.* (2011) and Wu *et al.* (2015). This requires early and extremely rapid assembly of these black holes, within the first billion years after the Big Bang, which poses a challenge to our current models of supermassive black hole (SMBH) formation and growth. One possible solution that has been proposed to alleviate this timing crunch is the formation of massive initial black hole seeds from the direct collapse of gas in pristine haloes in the cosmological context (Lodato & Natarajan (2006)). This new channel likely operates in addition to the standard one that leads to the formation of seeds from the remnants of the first stars. The first generation of stars referred to as Population III (Pop III hereafter) form from H_2-cooled, pristine gas at $z \sim 25$ onward. The initial mass function for Pop III stars is expected to be skewed high, resulting in the production of remnant black hole seeds with $M_{\bullet,III} \sim 100$ $M_\odot$. Under optimal conditions, these seeds could potentially grow via Eddington limited accretion to produce the SMBHs that power the detected high redshift quasars. This mechanism however requires extremely optimistic conditions post seed-formation: steady accretion from a large gas reservoir in the vicinity, and simultaneously, inefficient radiation feedback from the rapidly growing seed (see e.g. Tanaka *et al.* 2012, Pacucci *et al.* 2015 & Park *et al.* 2016). Additionally, the initial mass function of Pop III stars is also poorly constrained at present, resulting in uncertainty in the masses of the Pop III remnants. Recent reviews that present details of these models can be found in Volonteri (2012), Natarajan (2014) and Latif & Ferrara (2016).

The tuning required to produce SMBHs from Pop III remnants led to the proposal of alternate models for the formation of more massive black hole seeds from the direct collapse of pristine gas. In the early universe conditions feasible for the production of

these direct collapse black holes (DCBHs), with initial masses of 10^{3-5} $M_\odot$ (see e.g. Eisenstein & Loeb (1995), Omukai (2001), Oh & Haiman (2002), Bromm & Loeb (2003), Koushiappas *et al.* (2004), Lodato & Natarajan (2006)) exist. This additional DCBH seed formation channel has been actively explored in the past decade. What is required for this channel to operate are physical processes that prevent fragmentation and hence star-formation in early gas, rich haloes. This suppression of cooling requires the dissociation of molecular hydrogen which is an efficient coolant. Photons in the Lyman-Werner band ($11.2 \leqslant h\nu \leqslant 13.6$ eV) from star-forming sources nearby can effectively destroy molecular hydrogen. Photons in this band can photo–dissociate H_2 via $H_2 + \gamma_{\rm LW} \rightarrow H + H$ (see e.g. Omukai *et al.* 2001). Atomic H is an inefficient coolant that can only cool gas down to 8000 K; H_2 instead can cool the gas down to $\sim$ 200 K. Therefore, DCBH collapse can occur feasibly in satellite halos in the vicinity of star-forming galaxies that are the source of external Lyman-Werner photons. The presence of an external radiation field from a neighboring early star-forming galaxy can prevent a pristine halo from forming further Pop III stars. This suppression could instead lead to the isothermal collapse of the gas at 8000 K to extremely high densities, causing a runaway process that leads to the formation of a DCBH seed with $M_{\bullet,DC} \sim 10^{4-5}$ $M_\odot$ (see e.g. Bromm & Loeb (2003), Lodato & Natarajan (2006), Begelman *et al.* (2006), Volonteri *et al.* (2008), Shang *et al.* (2010), Johnson *et al.* (2012)Johnson, Whalen, Fryer, & Li, Ferrara *et al.* (2014)). Given their large initial seed masses, these DCBHs can grow and produce SMBHs by $z \sim 7$ even accreting at sub–Eddington rates.

There has been much recent progress in exploring the formation of these DCBH seeds, their environment, and their early growth history (Volonteri *et al.* (2008), Natarajan (2014), Agarwal *et al.* (2012), Agarwal *et al.* (2016), Pacucci & Ferrara (2015), Pacucci *et al.* (2015)). Current work suggests that the lighter Pop III remnant seeds and massive seeding models (DCBHs) can in principle be distinguished with multi-wavelength data at high redshift. This discrimination is possible due to the fact that DCBH seeds that assemble in satellite halos transit through a unique, short-lived stage post-formation upon merging with their parent haloes. During this stage, which we refer to as Obese Black hole Galaxies (OBGs), this first merger produces a source in which the black hole mass exceeds that of the acquired stellar component (Agarwal *et al.* 2013). This is in sharp contrast to what is seen locally, where the stellar masses of the bulges of nearby galaxies vastly exceeds that of the black hole harbored in the galactic nucleus (Tremaine *et al.* (2002), Ferrarese & Merritt (2000)). In addition at high redshifts, what is key is that the accretion luminosity of the growing black hole exceeds that of the stellar component. Therefore, calculating the shape of the emergent spectrum from accretion at these early epochs, we find that OBGs are potentially detectable with instruments aboard the upcoming *JWST* mission due to their distinct signatures in near and mid-infra-red wavelengths spanning 1 - 28 microns (Natarajan *et al.* 2016) .

2. The formation of direct collapse black holes

Physical conditions that permit the formation of DCBHs are available amply in the early universe (Agarwal *et al.* 2012). The host halos where DCBHs form are mini-halos with a virial temperature of $2000 < T < 10^4$ K. As outlined above, star formation in these haloes could be delayed or even halted by a modest level of external LW radiation field (Machacek *et al.* (2001), O'Shea & Norman (2008)), keeping them pristine till they grow to the atomic cooling limit $T \sim 10^4$ K. At this juncture, if the external LW radiation field prohibits molecular hydrogen formation by dissociation of H_2 (into H), DCBH formation would ensue due to the suppression of H_2 cooling and inhibition of fragmentation into

https://doi.org/10.1017/S174392131700076X Published online by Cambridge University Press

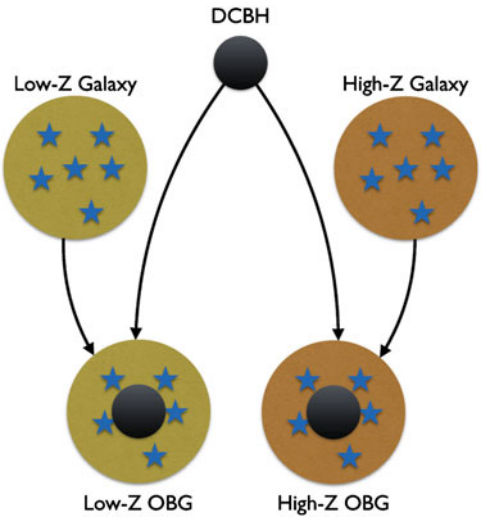

Figure 1. Schematic figure showing the DCBH seed formation scenario explored here. DCBH seeds form at the center of pristine, satellite halos that are illuminated by a nearby SF galaxy. Star formation is quenched in these DCBH host halos, although a stellar component is accrued promptly via merging with nearby SF galaxies. In the models studied here, we examine the growth following the merger of the DCBH (initial seed mass of 10^5 $M_\odot$) with a high and low metallicity stellar population. The gas in the post-merger halo is assumed to have the same metallicity as the stellar population. We also explore subsequent growth via accretion from a standard thin disk accretion as well as a radiatively inefficient slim disk.

stars. Viable sites are satellite halos in the vicinity of the first generation of star forming (SF) galaxies in the early universe (Agarwal *et al.* (2013), Agarwal *et al.* (2014)). At these satellite sites, pristine gas-rich proto-galactic disks could form that do not fragment or cool but rather go dynamically unstable (Q-unstable, as suggested by Toomre (1964), leading to rapid runaway accretion of gas to the center and to the formation of a massive DCBH seed. The physics and evolution of this process has been calculated analytically by Lodato & Natarajan (2006), and conducive conditions (assembly of massive proto-galactic disks) are increasingly seen to occur in state of the art high-resolution cosmological simulations of early structure formation as noted by Regan & Haehnelt(2009), Choi *et al.* (2013) and Latif *et al.* (2013). It is estimated that the typical masses of these DCBH seeds would lie in the range 10^{4-5} $M_\odot$ and the collapse process would be limited entirely by the mass available in the gas reservoir (e.g. Johnson *et al.* (2012)Johnson, Whalen, Fryer, & Li & Park *et al.* (2016)). Radiative feedback from these assembling DCBH seeds would halt SF in these halos (Aykutalp *et al.* 2014). Recently, Pacucci *et al.* (2015) have shown that $> 90\%$ of the gas in these proto-galactic core regions would be accreted and the rest blown away in $T_{\rm vir} \sim 10^4$ K DCBH host halos, under radiatively inefficient conditions.

Tracking the merging histories of these early dark matter halos, we find that these DCBHs' host satellite halos rapidly merge with the parent SF halo in their vicinity. This leads to the swift acquisition of a stellar component by the DCBH halo. This new object corresponds to the formation of a special transitory class of galaxies that we have referred to as OBGs (Agarwal *et al.* 2013). This is under the assumption that star formation is halted or highly suppressed in the DCBH halo itself due to radiative feedback from the assembling seed. Meanwhile, post-merger, stars and the DCBH continue to grow self consistently in an OBG in the sense that the same gas reservoir likely feeds the BH and

https://doi.org/10.1017/S174392131700076X Published online by Cambridge University Press

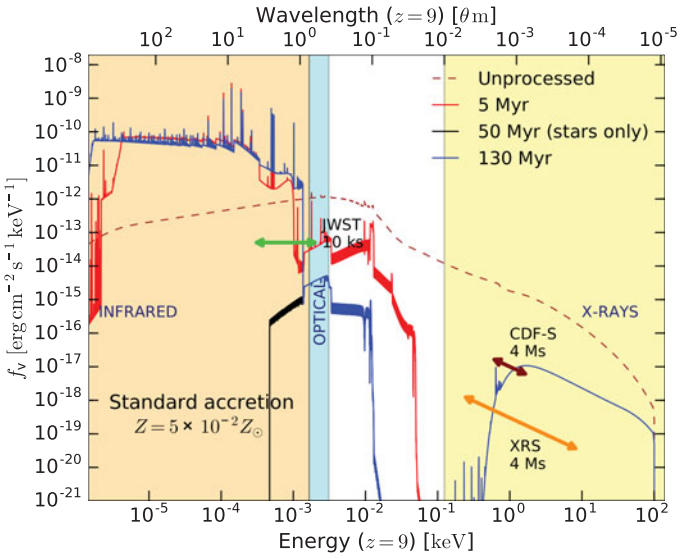

Figure 2. The computed multi-wavelength OBG spectrum for growth via standard accretion for an initial 10^5 $M_\odot$ DCBH seed, the higher metallicity case (0.05 $Z_\odot$) is plotted at two time slices $t = 5$ Myr and $t = 130$ Myr. The sensitivity limits for *JWST* for a 10 ks observation, the CDF-S (4 Ms) and the *X-ray Surveyor* (4 Ms) are highlighted. For contrast, we over-plot the spectrum of just the stellar component at a time slice $t = 60$ Myr (the high metallicity case).

forms stars in the merged remnant during this transient stage (see Fig. 1 for a schematic representation of the scenario explored here). For galaxies that host a rapidly growing DCBH seed, the energy output from BH accretion vastly exceeds the emission from the stellar component. In what follows, we outline the computation of the multi-wavelength SED of an OBG under these specific circumstances.

3. Calculating JWST signatures of DCBHs

We compute the multi-wavelength spectral energy distribution (SED) template for a growing DCBH seed in the OBG stage using a synthetic model to calculate the combined contribution of fluxes from the stellar and the accreting black hole components. We assemble these two components in the context of the merging hierarchy of LCDM halos and a background LW radiation field using the self-consistent prescription developed in Agarwal *et al.* (2012). Once a DCBH forms, its subsequent growth and energy output from accretion are simulated using a state–of–the–art 1D radiation-hydrodynamic code *GEMS*. This code simulates the spherical accretion onto a high-redshift black hole seed, computing the emitted luminosity self-consistently from the accretion rate. The full spectral analysis is then performed in a post-processing step with the code *Cloudy* Ferland *et al.* (2013). A full description of *GEMS* is available in Pacucci & Ferrara (2015). The growth and resulting energy output for the DCBH seed are modeled in two limiting cases. In the first, that we refer to as the *standard* case the growth involves accretion via a classic α-disk (Shakura & Sunyaev 1976), which is geometrically thin and optically thick. This accretion disk is radiatively efficient and accretion occurs, on average, at the Eddington rate. As described in Pacucci *et al.* (2015), this regime is entirely feedback-limited and the growth of the DCBH seed gets stunted once the feedback from the accretion process heats the gas, as it disrupts the inflow. In addition to this BH growth mode, we also model the case of radiatively inefficient accretion via a *slim disk* as proposed

https://doi.org/10.1017/S174392131700076X Published online by Cambridge University Press

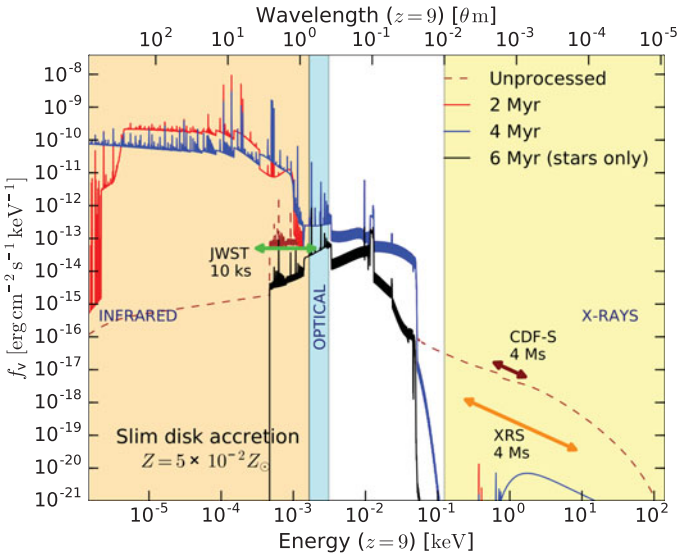

Figure 3. Here we show the spectrum with initial DCBH seed mass of 10^5 $M_\odot$, but now for growth via slim disk accretion for the higher metallicity case (0.05 $Z_\odot$) at two time slices $t = 2$ Myr and $t = 4$ Myr. Once again for contrast, we over-plot the spectrum of just the stellar component at a time slice of $t = 3$ Myr (high metallicity). The reference sensitivity limits for for *JWST*, the CDF-S and the *X-ray Surveyor* are highlighted here as well.

by Paczynski & Abramowicz (1982) and Abramowicz *et al.* (1988), and more recently explored in Sadowski (2009), and McKinney *et al.* (2014). In this case, radiation pressure is less efficient in quenching the gas inflow, due to photon trapping. Therefore, highly super-Eddington accretion rates may be reached and the mass growth is now entirely gas supply limited. We study the accretion of metal-enriched gas onto the DCBH during the OBG stage, where the metallicity is indexed to that of the merged stellar population. At this point, growth of the DCBH is jump-started by the merger. For the two modes of accretion outlined above, we explore the case of the higher metallicity for the OBG stage with $Z = 5\times10^{-2}\ Z_\odot$. The stellar population that merges to form the OBG is aged accordingly, with the metallicity of 5×10^{-2} $Z_\odot$ and an age of 800 Myr attributed to older Pop II stars. To model the stellar SED component of the OBG stage, we used *Yggdrasil*, a stellar population synthesis code that employs Raiter *et al.* (2010) for the lower metallicity, and *Starburst99* Leitherer *et al.* (1999) with Geneva high mass-loss tracks for the higher metallicity case. The nebular emission component was computed using *Cloudy* adopting the parameters described in Zackrisson *et al.* (2011). The SEDs were then rescaled to the Kroupa (2001) stellar initial mass function. The nebular emission is also computed assuming the same ambient gas metallicity as that of the stars. We model the post–merger star formation in the OBG host halo with a constant star formation rate, producing a final stellar mass of $M_* = 10^7$ $M_\odot$ at the end of the OBG phase. The total duration of the OBG phase varies from ~ 10 Myr in the slim disk cases to ~ 100 Myr in standard accretion cases. Detailed treatment and additional results are presented in Natarajan *et al.* (2016). Here we plot the output OBG spectra for the high-metallicity case in Figs. 2 and 3.

The emergent spectrum from our fiducial OBGs shows distinct observational signatures wherein UV photons are reprocessed by the gas as infra-red emission primarily between 1 - 30 microns. Therefore, we expect *JWST* to be particularly efficient in finding OBGs. We show the template infra-red spectra, observable in the *JWST* NIRCAM and MIRI bands

https://doi.org/10.1017/S174392131700076X Published online by Cambridge University Press

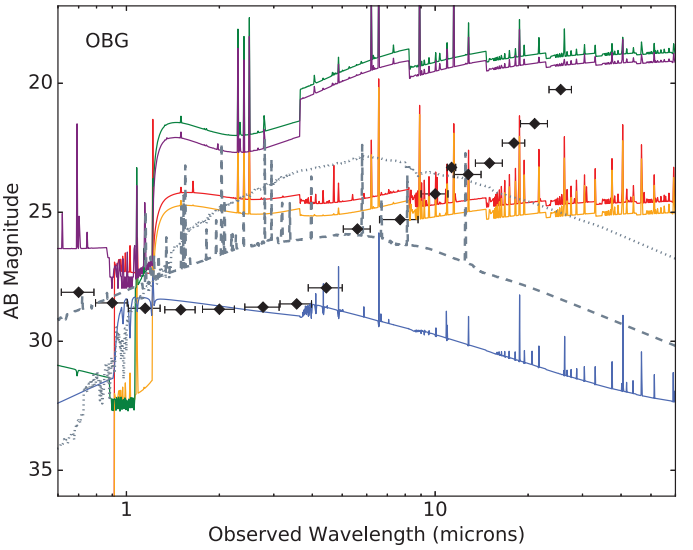

Figure 4. Predicted *JWST* template spectra for the DCBH seeding model and other contaminating high and low redshift sources. For this seeding model, the SED snapshots with the maximum-IR flux have been selected for plotting here. An OBG with an active DCBH accreting in the standard and slim disk cases for high and low metallicity at $z = 9$ are plotted. Here, for standard accretion the high metallicity case is shown in green; and the low metallicity case in red. In the slim disk accretion case, the lower metallicity template is plotted in orange and the higher one in purple. For comparison with potential contaminants, the spectrum of a typical actively star-forming high redshift galaxy (blue); and the measured spectra for low-redshift interlopers - an old and dusty star forming galaxy (grey dotted) at $z = 2.5$ and an Extreme Emission Line Galaxy (EELG) at $z = 2.1$ (grey, dashed) taken from Oesch *et al.* (2016) are over-plotted. The black symbols correspond to the MIRI and NIRCAM filter band passes on *JWST* and the error bars denote the width of the filters.

for both accretion modes in Fig. 4. We note the following trends: increasing the metal content of the host halo modifies the emerging spectrum in two ways: (i) it increases the absorption of high-energy ($\gtrsim 1$ keV) photons, and (ii) increases the power irradiated in the infra-red. From the calculated overall normalization of the spectrum, OBGs have estimated bolometric luminosities that are a factor of 100 or so higher than that of their growing Pop III seed counter-parts. We grow DCBH seeds to the final mass $\sim 10^7$ $M_\odot$, which is the total gas mass in the original halo. For a given BH seed mass, any change in the accretion model and in the metallicity essentially amounts to a re-scaling of the total growth time needed to arrive at the final mass. The effects of changing metallicity and accretion model are, in fact, degenerate. The reason is that we obtain the same high energy absorption with a small column of high metallicity gas or with a large, obscuring column of lower metallicity gas. The metallicity of the halo gas therefore changes the overall energy distribution due to photon scattering. A higher metallicity corresponds to an enhancement in the number of low-energy photons as higher energy photons with $E > 1$ keV are preferentially absorbed. There is also an enhancement in the re-radiated photons in the infra-red bands due to higher order Auger-like processes. Regardless of the metallicity of the stellar population which is also the adopted metallicity for the halo gas, the luminosity of the stellar population is always sub-dominant for the DCBH seeds. Aside from the discrimination offered by OBG candidate spectra in infra-red wavelengths, there are also clear signatures in X-ray wavelengths that we discuss further in Natarajan *et al.* (2016). OBG candidates as we show in Fig. 4 are easily detected in the MIRI bands.

https://doi.org/10.1017/S174392131700076X Published online by Cambridge University Press

These candidates would be characterized by a red slope between 1 and 10 microns and a flat slope beyond. This is in contrast to interloping low redshift sources that are extremely blue in the far IR as seen in Fig. 4 (Oesch *et al.* 2016).

4. Conclusions

Summarizing our results, for a growing DCBH seed with initial mass $M_{\rm seed} \sim 10^5$ $M_\odot$, we find that for the standard (Eddington–limited) growth, the signatures of the OBG stage are particularly distinct for the high metallicity case, as the overall infra-red flux is elevated relative to the lower metallicity case by about two orders of magnitude. We have shown the spectrum for the higher metallicity case here in Fig. 2. However, the X-ray flux is significantly higher for the lower metallicity case (discussed in detail in Natarajan *et al.* 2016). Despite their lower X-ray fluxes, the higher metallicity OBGs will be clearly detected in the NIRCAM and MIRI bands as seen in Fig. 4. For accretion via a slim–disk (super-Eddington growth), which is relatively short lived (5-10 Myr), OBGs would have diminished X-ray emission, and enhanced flux in the infra-red for the higher metallicity case shown here in Fig. 3. Due to the overall lowered X-ray flux though, detection will require deeper X-ray exposures than the ones currently available in the *Chandra* archive. Once again, despite their lower X-ray fluxes, the higher metallicity OBGs accreting via slim disks will also be detected unambiguously in the MIRI bands. In the context of the fiducial models studied here, high and low metallicity OBGs that are growing either via standard accretion or slim disk accretion will be unambiguously detected photometrically by *JWST* in the MIRI and NIRCAM bands. Additionally due to their high luminosities in the infra-red bands, OBGs could be feasibly followed up spectroscopically by NIRSPEC. Therefore, the upcoming *JWST* mission promises to provide new insights into the formation of the first black holes in the early universe and help discriminate between initial seeding models.

Acknowledgments

PN acknowledges support from a Theoretical and Computational Astrophysics Network grant with award number 1332858 from the National Science Foundation. She is grateful to her collaborators on this work: Fabio Pacucci, Andrea Ferrara, Bhaskar Agarwal, Angelo Ricarte, Erik Zackrisson and Nico Cappelluti.

References

Abramowicz, M. A., Czerny, B., Lasota, J. P., & Szuszkiewicz, E. 1988, *ApJ*, 332, 646
Agarwal, B., Dalla Vecchia, C., Johnson, J. L., Khochfar, S., & Paardekooper, J.-P. 2014, *MNRAS*, 443, 648
Agarwal, B., Davis, A. J., Khochfar, S., Natarajan, P., & Dunlop, J. S. 2013, *MNRAS*, 432, 3438
Agarwal, B., Johnson, J. L., Zackrisson, E., *et al.* 2016, *MNRAS*, 460, 4003
Agarwal, B., Khochfar, S., Johnson, J. L., *et al.* 2012, *MNRAS*, 425, 2854
Agarwal, B., Smith, B., Glover, S., Natarajan, P., & Khochfar, S., 2016, *MNRAS*, 459, 4209
Aykutalp, A., Wise, J. H., Spaans, M., & Meijerink, R. 2014, *ApJ*, 797, 139
Basu-Zych, A. R., Lehmer, B. D., Hornschemeier, A. E., *et al.* 2013, *ApJ*, 762, 45
Begelman, M. C., Volonteri, M., & Rees, M. J. 2006, *MNRAS*, 370, 289
Bromm, V. & Loeb, A. 2003, *ApJ*, 596, 34
Cappelluti, N., Comastri, A., Fontana, A., *et al.* 2016, *ApJ*, 823, 95
Choi, J.-H., Shlosman, I., & Begelman, M. C. 2013, *ApJ*, 774, 149
Decarli, R., Walter, F., Yang, Y., *et al.* 2012, *ApJ*, 756, 150

Devecchi, B. & Volonteri, M. 2009, *ApJ*, 694, 302
Dijkstra, M., Ferrara, A., & Mesinger, A. 2014, *MNRAS*, 442, 2036
Eisenstein, D. J. & Loeb, A. 1995, *ApJ*, 443, 11
Fan, X., *et al.* 2001, *AJ*, 122, 2833
Ferland, G. J., Porter, R. L., van Hoof, P. A. M., *et al.* 2013, Revista Mexicana de Astronomia y Astrofisica, 49, 137
Ferrara, A., Salvadori, S., Yue, B., & Schleicher, D. 2014, *MNRAS*, 443, 2410
Ferrarese, L. & Merritt, D. 2000, *ApJ Letters* 539, L9
Guo, Y., Ferguson, H. C., Giavalisco, M., *et al.* 2013, *ApJ Supplement*, 207, 24
Häring, N. & Rix, H.-W. 2004, *ApJ*l, 604, L89
Johnson, J. L., Whalen, D. J., Fryer, C. L., & Li, H. 2012, *ApJ*, 750, 66
Kormendy, J. & Ho, L. C. 2013, *ARAA*, 51, 511
Koushiappas, S. M., Bullock, J. S., & Dekel, A. 2004, *MNRAS*, 354, 292
Kroupa, P. 2001, *MNRAS*, 322, 231
Latif, M. A. & Ferrara, A. 2016, *PASA*, 33, 51
Latif, M. A., Schleicher, D. R. G., Schmidt, W., & Niemeyer, J. 2013, *MNRAS*, 433, 1607
Leitherer, C., Schaerer, D., Goldader, J. D., *et al.* 1999, *ApJ*s, 123, 3
Lodato, G. & Natarajan, P. 2006, *MNRAS*, 371, 1813
—. 2007, *MNRAS*, 377, L64
Machacek, M. E., Bryan, G. L., & Abel, T. 2001, *ApJ*, 548, 509
McKinney, J. C., Tchekhovskoy, A., Sadowski, A., & Narayan, R. 2014, *MNRAS*, 441, 3177
Mortlock, D. J., Warren, S. J., Venemans, B. P., *et al.* 2011, *Nature*, 474, 616
Natarajan, P., *et al.* 2016, *preprint, arXiv:1610.05312*
Natarajan, P., 2014, General Relativity and Gravitation, 46, 1702
Natarajan, P. & Volonteri, M. 2012, *MNRAS*, 422, 2051
Oesch, P. A., Brammer, G., van Dokkum, P. G., *et al.* 2016, *ApJ*, 819, 129
Oh, S. P. & Haiman, Z. 2002, *ApJ*, 569, 558
Omukai, K. 2001, *ApJ*, 546, 635
O'Shea, B. W. & Norman, M. L. 2008, *ApJ*, 673, 14
Pacucci, F. & Ferrara, A. 2015, *MNRAS*, 448, 104
Pacucci, F., Ferrara, A., Grazian, A., *et al.* 2016, *MNRAS*, 459, 1432
Pacucci, F., Ferrara, A., Volonteri, M., & Dubus, G. 2015, *MNRAS*, 454, 3771
Pacucci, F., Volonteri, M., & Ferrara, A. 2015, *MNRAS*, 452, 1922
Paczynski, B. & Abramowicz, M. A. 1982, *ApJ*, 253, 897
Park, K., Ricotti, M., Natarajan, P., Bogdanović, T., & Wise, J. H. 2016, *ApJ*, 818, 184
Raiter, A., Schaerer, D., & Fosbury, R. A. E. 2010, *Astronomy & Astrophysics*, 523, A64
Regan, J. A. & Haehnelt, M. G. 2009, *MNRAS*, 396, 343
Sadowski, A. 2009, *ApJ Supplement*, 183, 171
Shakura, N. I. & Sunyaev, R. A. 1976, *MNRAS*, 175, 613
Shang, C., Bryan, G. L., & Haiman, Z. 2010, *MNRAS*, 402, 1249
Tanaka, T., Perna, R., & Haiman, Z. 2012, *MNRAS*, 425, 2974
Toomre, A. 1964, *ApJ*, 139, 1217
Tremaine, S., Gebhardt, K., Bender, R., *et al.* 2002, *ApJ*, 574, 740
Volonteri, M. 2012, *Science*, 337, 544
Volonteri, M., Lodato, G., & Natarajan, P. 2008, *MNRAS*, 383, 1079
Wu, X.-B., Wang, F., Fan, X., *et al.* 2015, *Nature*, 518, 512
Zackrisson, E., Rydberg, C.-E., Schaerer, D., Östlin, G., & Tuli, M. 2011, *ApJ*, 740, 13